ROTOR BEARING SOLUTIONS INTERNATIONAL, LLC

www.rotorsolution.com

Rotor Drop Analyses and Auxiliary Bearing System Optimization for AMB Supported Rotor/Experimental Validation - Part I: Analysis Method

Prepared by:

RBSI Team

Jianming Cao, Paul Allaire, Tim Dimond

University of Potchefstroom, South Africa

Janse van Rensburg

Cerobear GmbH Christian Klatt

Rotor Bearing Solutions International, LLC

3277 Arbor Trace

Charlottesville, VA 22911

September 16, 2017

Rotor Drop Analyses and Auxiliary Bearing System Optimization for AMB Supported Rotor/Experimental Validation - Part I: Analysis Method

Jianming CAO*, Paul ALLAIRE*, Timothy DIMOND*, JJ. Janse van RENSBURG** and Christian KLATT***

*Rotor Bearing Solutions International, Charlottesville, VA 22911 USA

E-mail: jianming.cao@rotorsolution.com

**School for Mechanical and Nuclear Engineering, North-West University of Potchefstroom, South-Africa

***CEROBEAR GmbH, Germany

Abstract

For rotors supported with active magnetic bearings (AMBs), the auxiliary bearing system (AUX) is needed to avoid potential severe internal damaging due to AMB loss power or overload. The evolution of auxiliary systems has been required by the American Petroleum Institute (API) using analytical or experimental methods. In part I of this paper, a detailed rotor drop transient analysis method including flexible shaft, rolling element bearing components, as well as flexible/damped supporting structures is given. Part 2 gives the experimental validation of the method with a test rig and model optimization. A finite element based flexible rotor model is used to indicate the shaft motion before the drop (operating conditions) and during the rotor drop event. Un-lubricated Hertzian contact models are used for the shaft and inner races, for balls and races. To avoid heavy time consumption, two different methods, which calculate the ball bearing contact loads, are discussed and the simulation results are compared. These models are applied to predict shaft-race-ball displacements and angular speeds, contact loads and ball bearing stresses during the drop for auxiliary bearings. This method also can be used to design and optimize the auxiliary bearing system as presented in the 2nd part of this paper, based upon the experimental testing results and validation.

Keywords : Rotor Drop, AMB, Auxiliary Bearing, Rotordynamics; Nonlinear Transient Analysis

1. Introduction

Compared to conventional mechanical bearings, AMBs have many advantages: supporting the high-speed rotor without any contact, mechanical friction or lubrication, controlling the rotor position and vibration levels through feedback. The properly designed auxiliary bearing system (AUX) or backup bearing system, however, is necessary to protect the critical machine components from direct contact with the rotor in event of loss of AMB power or overload (Schweitzer, G. and Maslen, E., 2009). Rolling element bearings are the most common solution for AUX due to low friction, load capability in both radial and thrust, and minimum volume. Rotor drop happens when the rotor suddenly loses suspension during operation and a very detailed evaluation of auxiliary bearing system is needed. The understanding and mathematical modeling of auxiliary bearings has been made a priority by the API using analytical or experimental methods (API 617 8Ed). Some previous testing of auxiliary bearings for AMB has been described (Hawkins etl, 2006, Ransom etl, 2009, and Rensburg, 2014). The main difference between conventional bearing and AUXs is that AUXs are consumable protective devices and must be replaced after a number of drops when damage occurs in the rolling element bearings. However, the analysis methods for handling the drop problem are nonlinear and that results in heavy computer modeling time consumption.

To more accurately describe rotor behavior, a full nonlinear time transient analysis of the flexible rotor with auxiliary system is approached in this paper, based on Cao, 2015, in which the rotor is supported with fluid bearing and squeeze film dampers. Typically, rolling element steady state analyses are based on constant bearing rotational speed

and fixed external applied load, and Hertzian contact stiffness and damping coefficients between raceway and ball, angular contact angle, and ball behaviors are then calculated (Noel etl. 2013).

2. Rotor Drop Model

The free body diagram for the horizontal rotor drop analysis is shown in Fig. 1. The model can be used for a vertical rotor by changing gravitational direction from vertical to horizontal direction. In the figure, M_1~M_3 are shaft modal mass/inertia matrices; K_m and C_m are the AMB equivalent stiffness and damping prior to the drop; K_{pm} is negative permanent magnet stiffness, if it is present; K_a and Ca are the AUX stiffness and damping, which are calculated at each time step with the format of AUX forces; and Ks and C_s are flexible support or backup bumper (BB) located outside of the outer races if they exist.

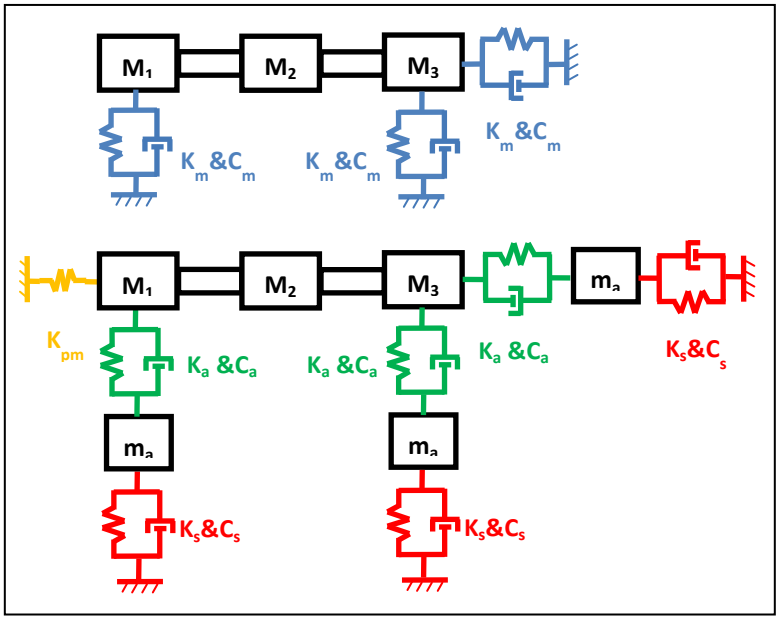

Fig. 1 Generic rotor drop analysis model - before (upper) and after (lower) drop

3. Equation of Motion

To calculate the lateral and torsional motion of rotor, a beam finite element with 12 degrees of freedom (DOF) is applied to model the linear shaft of the complex rotor system based on the finite element (FE) method with a fixed (non-rotating) frame as given by Cao, 2015. Here, x and y are the lateral coordinates and z is the axial coordinate. For a horizontal rotor, gravitational direction is negative y; and for a vertical rotor, it is positive z.

The shaft is assumed to be axially symmetric and modeled with Timoshenko beam elements. The built on components are modeled as lumped masses plus their associated polar and transverse mass moments of inertia. Additional rigid body models with 6 DOF for inner race and outer race are added for AUXs to simulate the race responses. AUXs are treated as nonlinear components where stiffness & damping effects are described by the bearing force equations and updated at each time step. Any other rotational speed and/or shaft nodal displacements/velocities, dependent external forces/torques, are also treated as nonlinear forces and have to be updated at each time step.

Two different motion equations, 1) before drop event (with AMB support, constant shaft rotational speed) and 2) after drop event (without AMB support, variable shaft rotational speed due to contact and friction), are first described. The system equations of motion before the drop event in generalized matrix form is:

$$M\ddot{u} + (C + \Omega G)\dot{u} + Ku = F_u(t,\Omega) + F_g + F_m(u,\dot{u},t) + T_e \tag{1}$$

And the system equations of motion after the drop event is:

$$M\ddot{u} + (C + \Omega G)\dot{u} + \left(K + \dot{\Omega} G\right)u = F_u(t,\Omega,\dot{\Omega}) + F_g + F_c(u,\dot{u},t) + T_e(t,\Omega) + F_b(u,\dot{u},t) + F_s(u,\dot{u},t) \tag{2}$$

where M, C, G, and K are the mass matrix of shaft and bearings, shaft damping matrix, shaft gyroscope matrix, and shaft stiffness matrix respectively; F_u, F_g, F_m, T_e, F_c, F_b, and F_s are the vectors of unbalance force, gravitational force due to rotor weight, AMB force, external torque, contact force, AUX force and flexible support force respectively. The relationship between nodal axial angle and rotational speed is $\dot{\theta}_{zj} = \Omega_j$; $j = 1,2,3\ldots$, which makes Eq. 2 a nonlinear equation of motion.

4. Shaft - Inner Race Contact Model

During the rotor drop event, there is possible radial contact between the shaft outside surface (or landing sleeve) and AUX inner race, and/or axial contact between the shaft touchdown shoulder and side surface of the inner race. Both types of contacts are considered in the analysis. Un-lubricated Hertzian line contact models and face contact models are applied to radial and axial contact separately with consideration of hard contact surfaces (Harris, 2007). The cross section of the radial contact model is shown in Fig. 2.

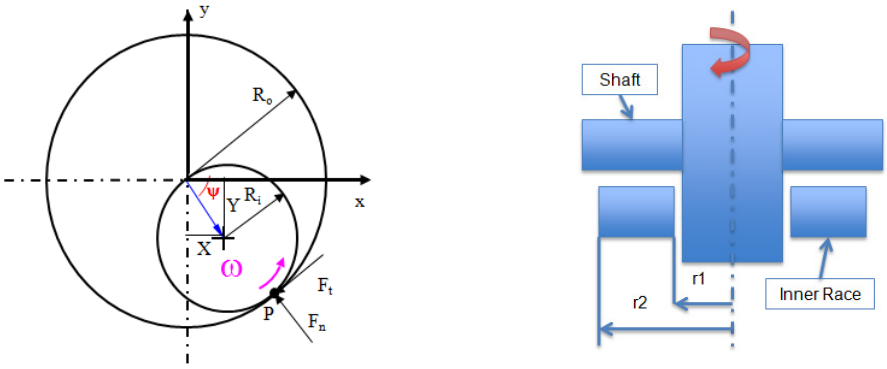

Fig. 2 Shaft - Inner race radial and axial contact model

The angle of the contact line of shaft and inner race is:

$$\psi = \tan^{-1}(Y/X) = \tan^{-1}(y_s - y_i / x_s - x_i) \tag{3}$$

where the subscripts s and i represent the shaft and the inner race. The nonlinear radial normal contact force relation is:

$$F_{nr} = K_{cr}\delta_r^{10/9} + C_{cr}\dot{\delta}_r \qquad \delta_r > 0 \tag{4}$$

where δ_r is the shaft/race deflection, which is given by:

$$\delta_r = \sqrt{X^2 + Y^2} - (R_0 - R_i) \tag{5}$$

Here X and Y are the shaft center location; R_0 and R_i are the radius of inner race and shaft. The Hertzian contact stiffness K_{cr} depends on the material properties and geometry of the rotor and inner race. For a given normal force, the deflection δ equation can be derived either by iterative method or by an analytical equation. An equation, for which an iterative computation is not necessary, is used here for given normal contact force Q (Palmgren, 1959):

$$\delta = 0.39\left[\frac{4(1-\nu_1^2)}{E_1} + \frac{4(1-\nu_2^2)}{E_2}\right]^{0.9} \frac{Q^{0.9}}{l^{0.8}} \quad \text{and} \quad K_{cr} = \frac{l^{\frac{8}{9}}}{0.39^{\frac{10}{9}}\left[\frac{4(1-\nu_1^2)}{E_1} + \frac{4(1-\nu_2^2)}{E_2}\right]} \tag{6}$$

where E_1, ν_1, E_2, ν_2 are Young's modulus and Poisson's ratio for two contact bodies, and l is the contact length.

The contact damping between surfaces is not linear and related to the deformation and material contact surfaces. The form used for the force equation, including both the Hertzian force and the damping force (Hunt etl. 1975) is:

$$Q = K_c\delta^n(1.5\eta\dot{\delta} + 1) = K_c\delta^n + (K_c\delta^n 1.5\eta)\dot{\delta} \tag{7}$$

Then the line contact damping coefficient C_{cr} can be expressed as:

$$C_{cr}=\begin{cases}K_c\delta_r^n 1.5\eta & K_c\delta_r^n 1.5\eta \le C_{\max}\\ C_{\max} & K_c\delta_r^n 1.5\eta > C_{\max}\end{cases} \tag{8}$$

where $K_c=K_{cr}$, $n=10/9$ for line contact, η is a value between 0.08 and 0.32 sec/m for steel or bronze. During the rotor drop event, large contact forces may occur, then large contact damping coefficients may be calculated through Eq. 10. However, the contact damping between two dry hard surfaces is small, so a limit of maximum contact damping is used in Eq. 10. In this paper, the maximum contact damping value is set to 500 N-sec/m for medium sized AUX bearings common in AMB systems.

The radial friction force and torque relations due to radial line contact are:

$$\begin{cases}F_{tr}=\mu_r F_{nr}\\ M_{cs}=-\mu_r F_{cr} R_0\\ M_{ci}=\mu_r F_{cr} R_i\end{cases} \text{ and } \mu_r=\begin{cases}\mu_k & v_s > v_i & \text{Kinetic}\\ \mu_s & v_s = v_i & \text{Static}\\ -\mu_k & v_s < v_i & \text{Kinetic}\end{cases} \tag{9}$$

where M_{cs} and M_{ci} are the friction torques applied to the shaft and to the inner race, μ_r is the friction coefficient depends on the velocities of the two bodies at the contacting line:

For axial surface contact situations, as shown in Fig. 2, the axial normal force F_{cz} has the format of the following equation:

$$F_{cz}=\begin{cases}K_{cz}\delta_{cz}+C_{cz}\dot{\delta}_{cz} & \delta_{cz}>0\\ 0 & \delta_{cz}\le 0\end{cases} \text{ and } K_{cz}=\begin{cases}\dfrac{E\sqrt{\pi\left(r_2^2-r_1^2\right)}}{0.96\left(1-\upsilon^2\right)} & r_2 > r_1\\ 0 & r_2 \le r_1\end{cases} \tag{10}$$

where δ_{cz} is the axial contact deflection between the shaft and inner race, r_2 is the landing face radius, and r_1 is the bore radius. The axial contact damping is calculated via a similar equation for in the radial direction (Eq. 10), but $K_c=K_{cz}$ and $n=1$ is used in Eq. 10. The torque due to the axial contact is obtained as:

$$M_{cz}=\int r dF_t=\int_{r1}^{r2}\int_0^{2\pi} r^2\mu_z\frac{F_{cz}}{A}d\theta dr=\mu_a R_{eq}F_{cz};\qquad R_{eq}=\begin{cases}\dfrac{2\left(r_2^3-r_1^3\right)}{3\left(r_2^2-r_1^2\right)} & r_2>r_1\\ 0 & r_2\le r_1\end{cases} \tag{11}$$

where μ_a is the friction coefficient; it has a similar definition to that in the radial direction. For surface contact situations, however, the rotational speed of the two bodies, not velocities of the contact points, are compared to evaluate the friction coefficients.

5. Auxiliary Bearing Model

In rotor drop simulations, the accurate prediction of ball bearing behavior is critical because the bearing behavior is significantly influenced by geometric relations, material properties, axial preload, inner race speed, and dynamic applied loads. In this paper, ball bearings without lubricant, as commonly used in AMB applications, are considered.

Steady state ball bearing models based on fixed external load under constant rotational speed have been presented by Noel elt, 2013. An iteration method is used to find ball equivalent position and then to obtain bearing stiffness under the given external load. For rotor drop analysis, the applied load due to contact depends upon interaction of shaft and the AUX bearing. Another issue for a time transient drop analysis is the heavy computer time consumption. However, most of those steady state theories and equations can be used in the nonlinear rotor drop model when suitable dynamic properties are included.

Assuming that the outer race geometric center is fitted at a fixed frame of reference (XYZ), the front view and cross section of an angular ball bearing is shown in Fig. 3. In the figure, only one example ball is shown. If the flexible support is installed onto the outer race, the relative displacements and velocities of the inner race and the balls to the outer race will be used. The position of the ball center and raceway groove curvature centers at normal angular position with and without applied load are shown in Fig. 4. All bearing balls subject to compressive normal forces contribute to forces acting on the inner race and outer race.

For a ball bearing without lubricant (dry or lubricant free bearing), the ball bearing contact forces applied onto the inner race and the outer race are:

$$\begin{cases} F_{Xi} = \sum_{j=1}^{Z_b}\left(Q_i\cos\alpha_i - \lambda_i\dfrac{M_g}{D_b}\sin\alpha_i\right)_j\cos\theta_j \\ F_{Yi} = \sum_{j=1}^{Z_b}\left(Q_i\cos\alpha_i - \lambda_i\dfrac{M_g}{D_b}\sin\alpha_i\right)_j\cos\theta_j \\ F_{Zi} = \sum_{j=1}^{Z_b}\left(Q_i\sin\alpha_i + \lambda_i\dfrac{M_g}{D_b}\cos\alpha_i\right)_j \\ M_{Zi} = f_b\sum_{j=1}^{Z_b}\left(Q_i\cos\alpha_i - \lambda_i\dfrac{M_g}{D_b}\sin\alpha_i\right)_j R_{ij} \end{cases} \text{ and } \begin{cases} F_{Xo} = \sum_{j=1}^{Z_b}\left(Q_o\cos\alpha_o - \lambda_o\dfrac{M_g}{D_b}\sin\alpha_o\right)_j\cos\theta_j \\ F_{Yo} = \sum_{j=1}^{Z_b}\left(Q_o\cos\alpha_o - \lambda_o\dfrac{M_g}{D_b}\sin\alpha_o\right)_j\cos\theta_j \\ F_{Zo} = \sum_{j=1}^{Z_b}\left(Q_o\sin\alpha_o + \lambda_o\dfrac{M_g}{D_b}\cos\alpha_o\right)_j \\ M_{Zo} = f_b\sum_{j=1}^{Z_b}\left(Q_o\cos\alpha_o - \lambda_o\dfrac{M_g}{D_b}\sin\alpha_o\right)_j R_{oj} \end{cases} \tag{12}$$

where Z_b is total number of balls in the bearing, M_{zi} and M_{zo} are friction torques about the bearing center due to the applied force, μ_b is the ball bearing friction coefficient, R_{ij} and R_{oj} are the radial distances of the bearing center to j^{th} ball contact points.

$$R_{ij} = \left(\frac{d_m}{2} + r_b - r_i - \frac{D_b}{2}\cos\alpha_i\right)_j; \quad R_{oj} = \left(\frac{d_m}{2} + r_b - r_o + \frac{D_b}{2}\cos\alpha_o\right)_j \tag{13}$$

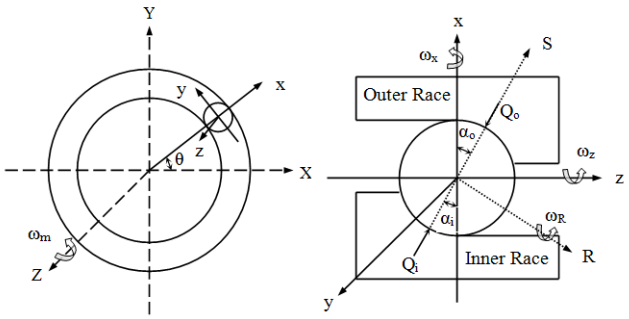

Fig. 3 Bearing Geometry and Coordinates

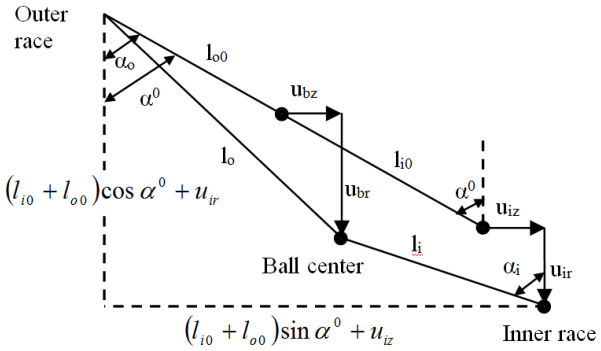

Fig. 4 Ball and Raceway Groove Curvature Centers

Finding the contact angle for each ball on the inner race and outer race using an iteration method at each time step takes more than 90% of calculation time in the simulation (see Table 1). The existence of the AUX air gap in both radial and axial directions makes the AUXs initially have zero or a very low rotating speed due to aerodynamic effects. The maximum bearing stress generally occurs during the first several touchdowns and at the same time the AUXs are angularly accelerated. Unless there is poor AUX design, the shaft-race contact force decreases very fast after first several touchdowns. The ball centrifugal forces and gyroscopic moments by themselves normally won't damage the bearing. If those forces and moments are neglected, the contact angles on inner and outer races for each ball are the same. The contact angle of each ball can be calculated directly based on the relative displacement and velocity of inner race and outer race and no iteration method is needed. The ball location and angular velocity, if needed, can be obtained directly at each time step.

Neglecting the ball centrifugal forces and gyroscopic moments, the direct method uses the following equations:

$$\begin{cases} \tan\alpha_i = \tan\alpha_o = \dfrac{l_0\sin\alpha^0 + u_{iz}}{l_0\cos\alpha^0 + u_{ir}} \\ l = \sqrt{\left(l_0\cos\alpha^0 + u_{ir}\right)^2 + \left(l_0\sin\alpha^0 + u_{iz}\right)^2} \end{cases} \tag{14}$$

$$\begin{cases} \delta_n = \delta_i + \delta_o = l - l_0 - \Delta \\ \dot{\delta}_n = \dfrac{\left(l_0\cos\alpha^0 + u_{ir}\right)\dot{u}_{ir} + \left(l_0\sin\alpha^0 + u_{iz}\right)\dot{u}_{iz}}{l} \end{cases} \tag{15}$$

where $\Delta = P_d/2$ for bearing without axial preload; $\Delta = 0$ for bearing with axial preload; $l_0 = r_i + r_o - D_b$.

The normal compressive force on the j^{th} ball considering damping effect is:

$$Q_n = Q_i = Q_o = k_n \delta_n^{3/2} + c_n \dot{\delta}_n \qquad \delta_n > 0 \tag{16}$$

where k_n is equivalent stiffness of the ball-raceway:

$$k_n = \left[\frac{1}{(1/k_i)^{2/3} + (1/k_o)^{2/3}} \right]^{3/2} \tag{17}$$

and c_n is damping coefficient with the expression:

$$c_n = \begin{cases} k_n \delta_n^{3/2} 1.5\eta & k_n \delta_n^{3/2} 1.5\eta \le C_{\max}/Z_b \\ C_{\max}/Z_b & k_n \delta_n^{3/2} 1.5\eta > C_{\max}/Z_b \end{cases} \tag{18}$$

where η is a value between 0.08 and 0.32 sec/m. The total forces applying to the inner and outer races are similar to Eq. 16&17, but use $M_g=0$. Since the contact angles on the inner race and outer race are same, there is no slippage friction torque or $M_{si}=M_{so}=0$.

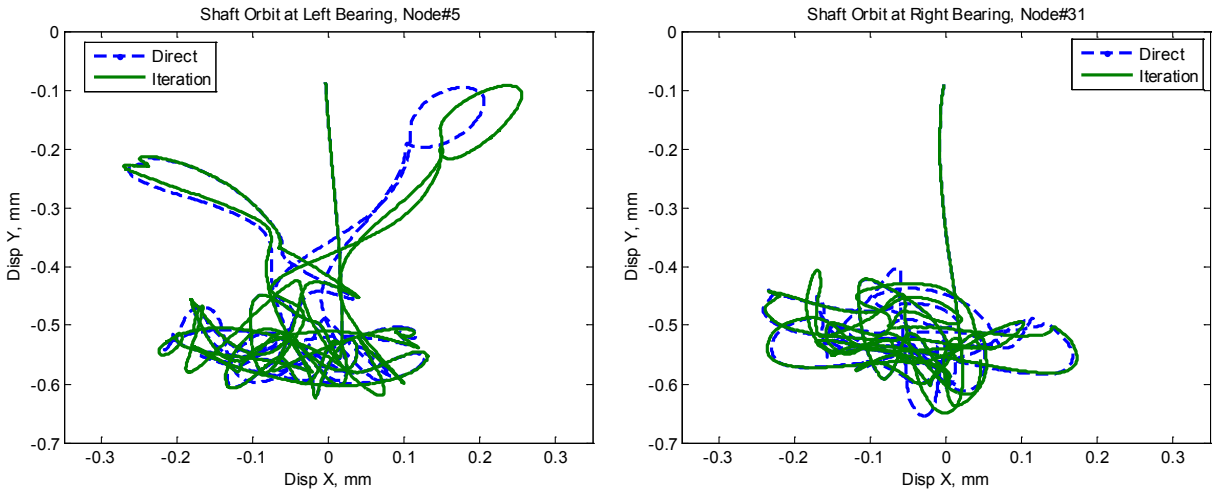

Figure 5 Compressor rotor orbits at left bearing and at right bearing

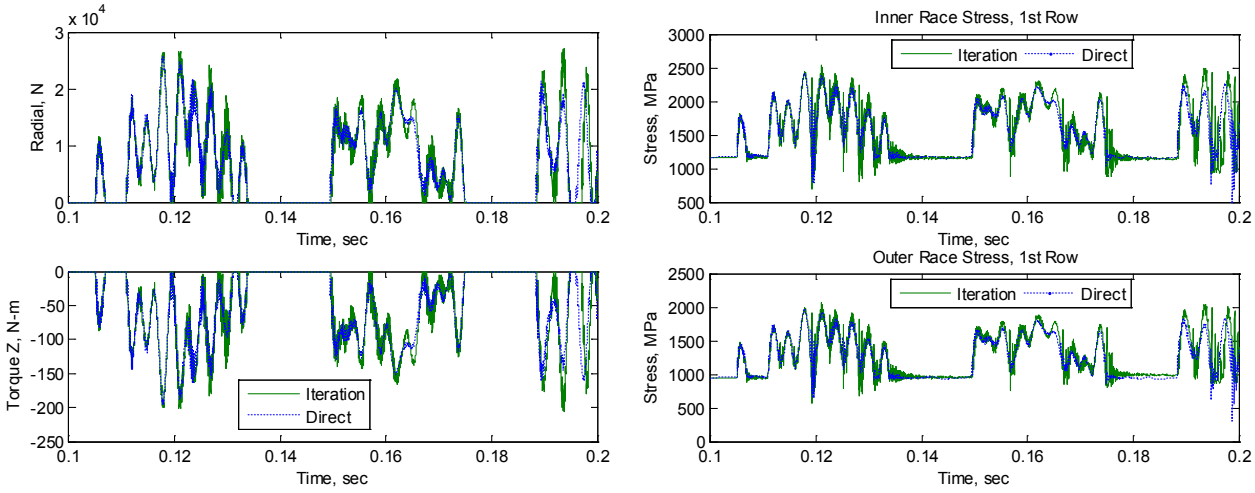

Figure 6 Compressor ball bearing contact forces and maximum bearing stresses at left bearing during rotor drop

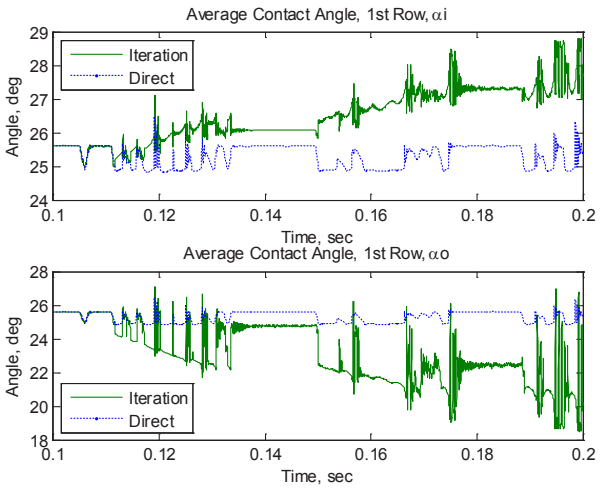

Fig. 7 Average contact angle at left bearing

Table 1 Computing Time Comparison

8-Stage Compressor, Period of 0.1sec., $\Delta t=4\times10^{-6}$ s	
Iteration Method	5950 sec
Direct Method	330 sec

The analysis results based on the two methods are compared first. A typical horizontal 8-stage centrifugal compressor radial drop analysis (the two radial AMBs and thrust AMB lose power at 0.1sec) is approached using two different methods. The detailed rotor description and model is given in Part II of the paper. Here only the analysis results using different methods are given for comparison purposes. As shown from the analysis results, the shaft orbits (Figs. 8), the contact force and the maximum bearing stress (Fig. 6) are reasonably close for both methods; the average contact angles of all the balls, however, are somewhat different, as shown in Fig. 7. With the radial contact loads and considering the bearing ball centrifugal forces, the contact angle on the outer race is less than that on inner race, as shown in Fig. 7. Table 1 gives the time consumption for the two methods. The direct method is 18 times faster than the iteration method. In the following rotor drop examples in this paper, only the direct method is used to save computing time. In this paper, the contact between balls or ball and cage (if they exist) has not been considered as the most commonly used AUX bearings used are cageless.

6. Axial Preloading And Initial Condition

A typical plot of bearing deflection vs. load is shown in Fig. 8. For duplex pairs of angular contact bearings, the total axial/thrust load is the difference of two bearings and the radial load is the sum of two bearings:

$$\begin{cases} F_r = F_{r1} + F_{r2} \\ F_a = F_{a1} - F_{a2} \end{cases} \quad \text{and} \quad \begin{cases} \delta_{a1} = \delta_p + \delta_a \\ \delta_{a2} = \begin{cases} \delta_p - \delta_a & \delta_p > \delta_a \\ 0 & \delta_p \le \delta_a \end{cases} \end{cases} \tag{19}$$

where δ_p is the axial deformation due to preload, δ_a is the axial deformation of the bearing due to external forces.

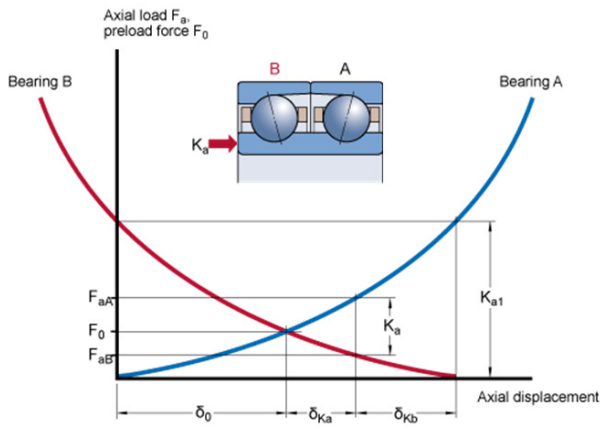

Fig. 8 Preloaded double row ball bearing

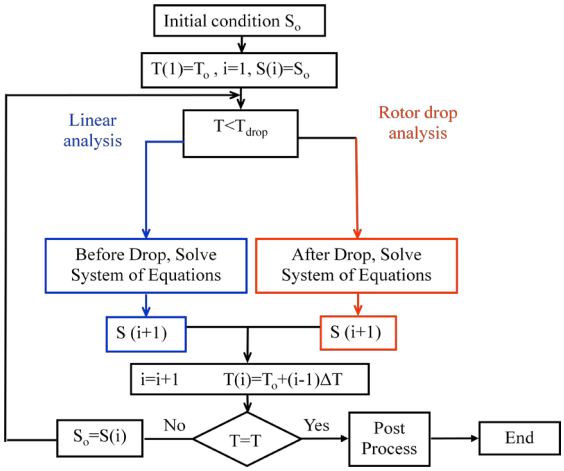

Fig. 9 Flow chart of rotor drop analysis

Figure 9 is a flowchart illustrating the calculation of the transient analysis. The following steps are used in the rotor drop analysis. First, we obtain the initial shaft nodal positions and velocities by solving motion equation before the rotor drop. Then the initial conditions of auxiliary bearing system are calculated based on the axial preload. We reassemble the mass, stiffness and damping matrices by choosing the AMB without electrical power, adding the auxiliary bearing and flexible support/damper if they exist. The transient analysis starts from the initial position of the rotor, the auxiliary bearings and the support system with the initial rotational speed, and then the bearing/support system forces and the external torques are calculated at the initial position. The new shaft position and velocity values are calculated, which are then used to update the bearing/support forces and the running speed at each time step. The last step is to save and to post-process the saved data. For time transient analysis, very large output files may generated.

6. Conclusions

This paper presents the detailed formulation of a nonlinear transient analysis for rotor drop event including the flexible shaft, the rolling element bearing components considering inner/outer races, balls, and flexible/damped supporting structures. Initial conditions are obtained through solving a linear rotor/AMB motion equation. A finite element based 6-DOF flexible rotor model is used to indicate shaft motion operating conditions before and after a rotor drop event. Un-lubricated Hertzian contact models are used for contacting between the shaft and the inner race, between the balls and the raceways. The time transient analyses are approached using the 4^{th} order Runge-Kutta method.

Two different approach methods in ball bearing contact model are discussed and the simulation results are compared. Two methods has similar response including shaft orbits, contact loads and maximum bearing stress except angular contact angles. The simulation results indicate that iteration method is much slower than direct method (same contact angles at each ball, but different balls have different contact angles), and the heavy time consumption makes the iteration method has difficulty in industrial applications but can be used if necessary. Part 2 of this paper concerns the experimental validation of this approach and optimization of the rotor drop model parameters.

References

Schweitzer, G. and Maslen, E., eds., 2009, "Magnetic Bearings: Theory, Design, and Application to Rotating Machinery", Springer-Verlag, Berlin

American Petroleum Institute, API Standard 617, 8ed, 2014, "Axial and Centrifugal Compressors and Expander-compressors for Petroleum, Chemical and Gas Industry Services",. Washington, D.C

Hawkins, L., Filatov, A., Imani, S., and Prosser, D., 2006, “Test Results and Analytical Predictions for Rotor Drop Testing of an AMB Expander/Generator,” ASME J. Eng Gas Turbines Power, vol. 129, pp. 522-529

Ransom, D., Masala, A., Moore, J., Vannini, G., and Camatti, M., 2009, “Numerical and Experimental Simulation of a Vertical High Speed Motorcompressor Rotor Drop onto Catcher Bearings” J. Sys. Design Dynamics, 3(4), pp. 596–606

Cao, J., Dimond, T. W., and Allaire P. E., 2015, "Coupled Lateral and Torsional Nonlinear Transient Rotor-Bearing System Analysis with Applications", ASME J. Dyn. Sys., Meas., Control, 137(9): 091011-091011-9

Palmgren, A., 1959, "Ball and Roller Bearing Engineering", 3rd ed., SKF industries, Burbank, Philadelphia

Harris, T. A., and Kotzalas, M. N., 2007, "Rolling Breaing Analysis: Essential Concepts of Bearing Technology", 5th Ed., Taylor & Francis Group, New York, NY

Harris, T. A., and Kotzalas, M. N., "Rolling Breaing Analysis: Advanced Concepts of Bearing Technology", 5th Ed., Taylor & Francis Group, New York, NY

Brewe, D. and Hamrock, B., 1977, "Simplified Solution for Elliptical-contact Deformation Between Two Elastic Solids", ASME Trans. J. Lub. Tech., 101(2), 231-239, 1977

Noel, D, Ritou, M., and Furet B., 2013, "Complete Analytical Expression of the Stiffness Matrix of Angular Contact Ball Bearings", ASME J. Tribo., 135(10), pp. 041101-041101-8.

Hunt, K. H., and Crossley, F. R. E., 1975, "Coefficient of Restitution Interpreted as Damping in Vibroimpact", ASME J. Appl. Mech, 42(2), 440-445